Science Advances
AAAS

Supplementary Materials for

Cell activity modulation and its specific function maintenance by bioinspired electromechanical nanogenerator

Tong Li, Chuanmei Shi, Fei Jin, Fan Yang, Long Gu, Ting Wang, Wei Dong, Zhang-Qi Feng*

*Corresponding author. Email: fengzhangqi1981@163.com

Published 24 September 2021, *Sci. Adv.* **7**, eabh2350 (2021)
DOI: 10.1126/sciadv.abh2350

This PDF file includes:

Supplementary Text

note S1. Fabrication of bio-NGs

We fabricated bio-NGs in three steps. First, highly discrete Fe_3O_4/PAN fibers were prepared. With the introduction of Fe_3O_4 magnetic nanopraticles, 3D scaffolds with micropore which is suitable for cell migration can be prepared by electrospinning and received by water with assistance of magnetic field, besides Fe_3O_4 can be relatively uniformly dispersed in the fibers. Specifically, the electrospinning solution was prepared by dissolving PAN powder (MW = 40 kDa, Binzhou Hengtai Chemical fiber Co., Ltd.) in a mixture solution of Fe_3O_4 (99.9%, Sigma-Aldrich) and DMF (Sinopharm Chemical Reagent Co., Ltd.) under sonication for 90 minutes. To check the influence of the ratio of Fe_3O_4 and PAN on the degree of dispersion, Fe_3O_4/PAN solutions (PAN/DMF, 0.15 g mL^{-1}) with different contents of Fe_3O_4 (0.03, 0.036, 0.039, 0.042 and 0.045 g mL^{-1}) were prepared. The loading contents of Fe_3O_4 in composites were calculated by the ratio of the loading amount of Fe_3O_4 to the total amount of PAN: 20, 24, 26, 28 and 30%. After the electrospinning, the prepared fiber was transferred into a 50 ml centrifuge tube and freeze-dried for 60 hours to obtain 3D Fe_3O_4/PAN scaffolds with different Fe_3O_4 content. Fe_3O_4/PAN fibers were fabricated under a suitable electrospinning environment (room temperature and relative humidity 35%). The laboratory setup consists of a spinneret connected to a high-voltage power supply, a syringe pump, and an 18 cm diameter petri dish with ultrapure water inside. The electrospinning process was operated at a feed rate of 0.5 mLh^{-1}, an applied voltage of 15 kV, and a distance between spinneret and collector of 15 cm. 26%-Fe_3O_4 PAN fibers yielded the highest average pore size value. Therefore, 26%-Fe_3O_4 PAN (named Fe_3O_4/PAN) fibers were selected as the first precursor for the fabrication of bio-NGs.

Second, PEDOT was polymerized *in situ* on 26%-Fe_3O_4 PAN fibers. The freeze-dried Fe_3O_4/PAN fibers were soaked in diethyl ether (AR, Sinopharm Chemical Reagent Co., Ltd.) solution of 3,4-ethylenedioxythiophene (EDOT, 99%, Shanghai Aladdin Biochemical Technology Co., Ltd.) and $FeCl_3$ (99.9%, Shanghai Aladdin Biochemical Technology Co., Ltd.). In order to screen out the best EDOT concentration, the EDOT/$FeCl_3$ solutions ($FeCl_3$/diethyl ether, 0.02 g mL^{-1}) with different contents of EDOT (3, 4, 5, 6, 7 mg mL^{-1}) were prepared. The *in situ* polymerization process was performed under ultrasonic ice water bath. The 5 mg mL^{-1}-EDOT Fe_3O_4/PAN (named PEDOT/Fe_3O_4/PAN) fibers gave the highest charge capacity value of

5.653E-6 C. Therefore, we chose this EDOT concentration as the second precursor for fabricating bio-NGs.

Third, GO was introduced on PEDOT/Fe_3O_4/PAN fibers by electrostatic adsorption. In the second step, PEDOT was obtained by *in situ* polymerization using $FeCl_3$ as an oxidant. In the polymerization process, EDOT often formed cationic radicals and then coupled to form long-chain polymers, so the surface of PEDOT was positively charged. While the surface of GO was rich in anionic groups such as carboxyl and hydroxyl groups, which can be electrostatically adsorbed with PEDOT, thereby self-assembled into GO outer layer. Briefly, the freeze-dried PEDOT/Fe_3O_4/PAN fibers were immersed in aqueous solution of GO (5 mg mL^{-1}) and shacking for 90 minutes to fully adsorb GO. Then, after standing for 24 hours, the unabsorbed GO was removed by washing with ultrapure water. Finally, the fibrous scaffold was freeze-dried for 40 hours to obtain the final 3D GO/PEDOT/Fe_3O_4/PAN fibers. These GO/PEDOT/Fe_3O_4/PAN fibers acted as bio-NGs for cell culture.

note S2. Finite element modeling of the cells on piezoelectric fibers in bio-NGs

The finite element simulation of the electrical properties for single fiber was conducted by the commercial software ANSYS. The fibers and living cell were modeled by piezoelectric element Solid227 and structural element Shell181, respectively. Two PAN fibers coupled with a living cell, and the two ends of the fiber were defined as an anchor or fixed constrain and a load force of 0.1-10 nN was applied at the cell-fiber interface.

note S3. Equivalent circuit model of NG-cell interaction

The membrane potential of a living cell was controlled by the inflow and outflow of ions. This type of interaction can be modeled by an electrical equivalent circuit using a voltage source, a resistor, and a capacitor. The capacitor represented the intracellular and extracellular charge concentrations, separated by the non-conducting cell membrane. This was a good approximation of a pure phospholipid bilayer which had an extremely high resistivity of about 10^{15} Ωcm^{-1}. The voltage source represented the initial typical potential that was maintained across the ion channels in the resting state. Finally, the current that flows through the resistor represents the quantity of ions allowed to flow in or out of the cell. Therefore, ion channels can be modelled by variable resistors. Then, an external electrical stimulation like the one produced by an electrode can be modeled by another voltage source that affects the voltage across the cell membrane, *i.e.* the capacitance. Because this electrode is normally inserted in the tissue, it can be located at a

certain distance to the cell under study. However, the cell is electrically stimulated through the contact interface between cell and stimulation electrode that can be represented as a resistor, R_{int}. In our case, the external voltage stimulation is generated by a NG (V_{NG}) when mechanically strained. The system equivalent circuit model is a simplified form of the more complex models using discrete membrane portions or different ion channels and pumps. This preliminary model is useful to observe how a voltage pulse can be transmitted to the cell membrane to activate ion channels, but the current and voltage values could not be fully accurate.

note S4. PFM characterizations of the single fiber in bio-NGs

Piezoelectric response measurement of the single fiber in bio-NGs was undertaken by PFM (Multimode 8, Bruker) in contact lithography mode. Single fiber was produced by the electrospinning jet and directly loaded on to the FTO conductive glass because of its high surface energy. Cantilevers (Econo-SCM-PIC, Asylum Research) with Cr/Pt conductive coating, tip radius below 25 nm and spring constant of 0.1 N m^{-1} were used for the PFM measurements. The PFM was carried out in contact lithography mode, whereby a potential was applied to the sample in pre-defined patterns and the amplitude and phase changes relative to the unbiased areas were observed. The voltage was swept in increments of approximately 0.2 V from -10 V to 10 V on each scan line, with a scan rate of 0.2 Hz. An AC excitation (V_{ac} = 1.6 V) riding on the DC bias voltage (V_{dc}) was applied between the tip and the bottom electrode. Dual AC resonance tracking (DART-PFM) was then undertaken at 1 Hz scan rate to ensure the stability of the material.

The maximum amplitude (A) was 810 pm. The effective d_{33} coefficient could be calculated by fitting the linear portion of the A curves as $A = d_{33}V_{dc}Q$, where Q represented the unitless quality factor of the cantilever resonance peak obtained during the PFM experiments, which in this case was consistent between 10 and 20 with slight variations between samples, and V represented the applied voltage.

note S5. Fabrication of 2D NGs

We directly electrospun low-density 26%-Fe_3O_4/PAN fibers on the round cover slides. Then, PEDOT (5 mg mL^{-1}) and GO (5 mg mL^{-1}) were successively introduced into the Fe_3O_4/PAN fibers to fabricate 2D NGs.

note S6. Fabrication of 3D fibers

3D fibers referred to 3D GO/PEDOT/Fe_3O_4/PLA fibers. The electrospinning solution was prepared by dissolving PLA (MW = 500 kDa, Daigang Biological Technology Co., Ltd.) in

dichloromethane mixed with Fe_3O_4 (PLA/dichloromethane = 4 wt%, Fe_3O_4: 0.039 g mL^{-1}) under stirring at 40 ℃ for 3 hours. The laboratory setup consists of a spinneret connected to a high-voltage power supply, a syringe pump, and an 18 cm diameter petri dish with ultrapure water inside. The electrospinning process was operated at a feed rate of 0.5 mL h^{-1}, an applied voltage of 10 kV. The other steps including introducing PEDOT and GO are the same as the above-mentioned preparing bio-NGs.

note S7. hMSCs morphology and their osteogenic differentiation

To observe the morphology and attachment of hMSCs on the fibers in bio-NGs, photographs of hMSCs after 14 days in culture were collected by laser scanning confocal microscope (SP8, Leica). To clearly observe the differentiation morphology of the cells, the hMSCs were fluorescently stained with fluorescein diacetate (FDA). FDA dye was excited with a 484 nm laser and observed under laser scanning confocal microscope.

The cell proliferation of hMSCs was assessed using DNA assay. The number of cells were collected on day 1, day 3, day 7 and day. To better quantify these substantial differences in cell spreading, we calculated the cell proliferation rate adhered to different scaffolds using DNA assay. The cell proliferation rate was obtained by dividing the adhered cells by the original seeded cells.

Bone alkaline phosphatase (ALP) was an ectoenzyme attached to the outer surface of the cell membrane of osteoblasts by glycosylphosphatidylinositol, which was generally considered to be sensitive and specific markers of bone formation. To confirm the osteoblastic differentiation, the activity of ALP was evaluated to investigate the differentiation patterns of hMSCs. The ALP was measured by using a cellular alkaline phosphatase assay kit (GenMed). A Pierce BCA Protein Assay kit (Thermo) was used to quantify the total cellular protein content. The ALP activity of each sample was normalized to the construct wet weight and BCA protein content, respectively.

Supplementary Figure

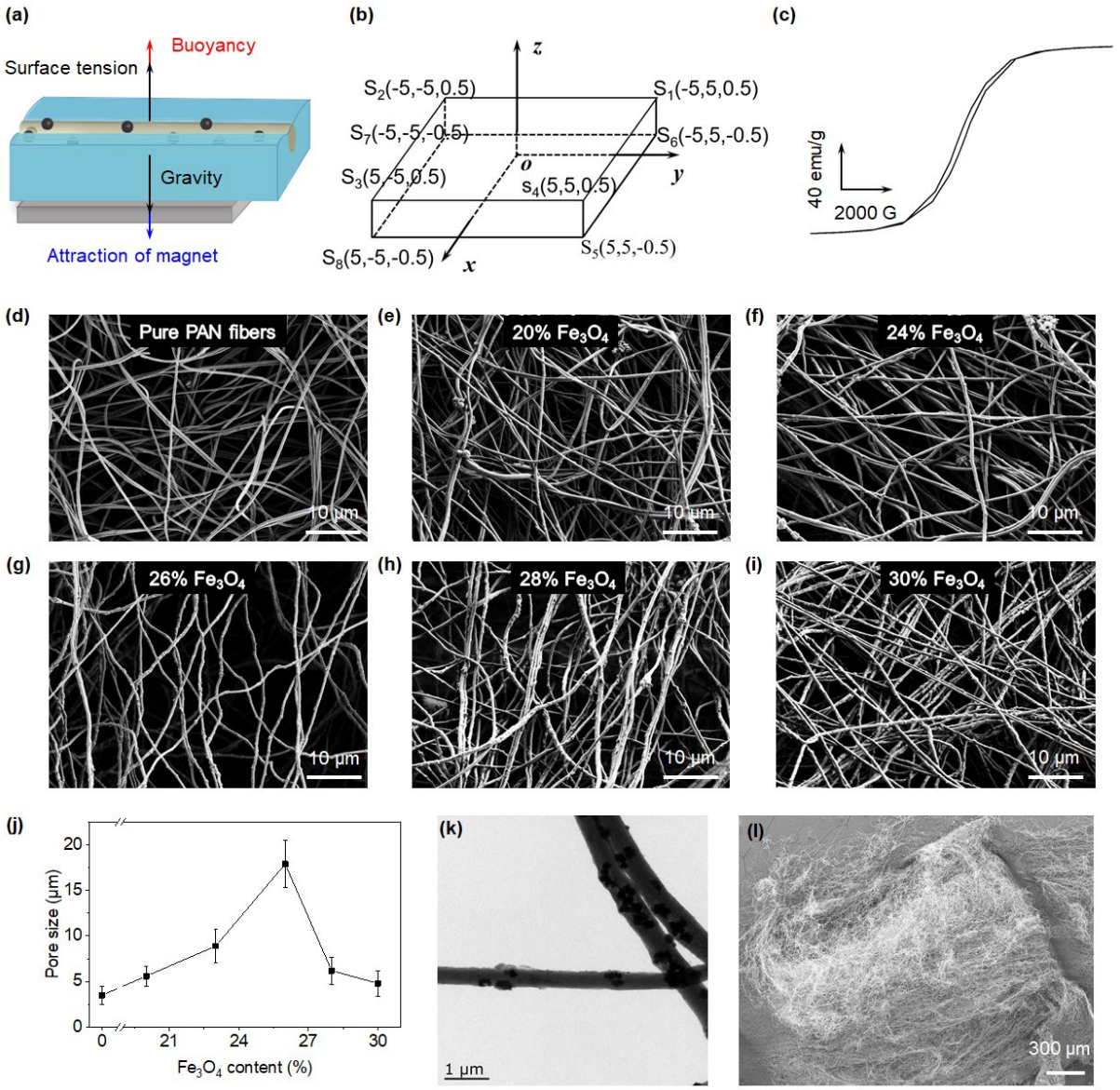

fig. S1. (a) Schematic diagram of the force of a single Fe_3O_4/PAN fiber on the water surface in a magnetic field. (b) The coordinate system of the square magnet. (c) Hysteresis loop of pure Fe_3O_4 nanoparticles. (d-i) SEM images of PAN fibers with different Fe_3O_4 contents. (j) Average pore size value as a function of the Fe_3O_4 content, counted from the SEM images using ImageJ software. (k) TEM image of 26%-Fe_3O_4 PAN fibers showing well-dispersed Fe_3O_4 nanoparticles. (l) Highly discrete and fluffy 26%-Fe_3O_4 PAN fibers.

Due to the inherent hydrophobicity of PAN, PAN fibers will be affected by huge surface tension (surface tension of water 72 mN m^{-1}, 25℃). This will result in the PAN fibers to accumulate on the water surface into a nano-plane fibrous membrane instead of highly discrete

fibrous scaffolds. Therefore, only by breaking through the surface tension and buoyancy of water can discrete PAN fibers be obtained. When Fe_3O_4 nanoparticles were incorporated, the neodymium iron boron magnet will attract Fe_3O_4-doped PAN fibers, causing the fibers to break these resistances (fig. S1a), thereby obtaining discrete fibers (26%-Fe_3O_4 PAN fibers, fig. S1k). To further illustrate the criticality of Fe_3O_4 magnetic nanoparticles, a single 26%-Fe_3O_4 PAN fiber with a length of 1 cm and a diameter of 600 nm was taken as an example. The weight of this single fiber was 4.132×10^{-8} mN. If it was assumed that the fiber just completely entered the water surface, the buoyancy of the fiber was 2.769×10^{-8} mN. On the other hand, according to Young's equation $\gamma_{lV}=\gamma_{sV}-\gamma_{sL}\times cos\theta$, it is known that the surface tension of PAN on the water surface was 0.0651 mN cm^{-1}, so the surface tension of 1 cm PAN fiber in an ideal state was 0.1302 mN. Then, without applying any external force, at least 9.552×10^{6} fibers need to be stacked to break through the surface tension. This will cause a lot of fibers to accumulate on the water. However, the introduction of magnetic field in this work can effectively address this issue. In this single 26%-Fe_3O_4 PAN fiber, the mass of magnetic nanoparticles was 8.7×10^{-10} g. The magnet we used was N52 neodymium iron boron magnet, and the calculation of magnetic field distribution was calculated by the following square magnetic field distribution equations (S1-3):

$$H_z=\frac{M}{4\pi}G(x,y,z) \quad \text{(Eq. S1)}$$

$$G(x,y,z)=g(s_1)+g(s_3)+g(s_5)+g(s_7)-g(s_2)-g(s_4)-g(s_6)-g(s_8) \quad \text{(Eq. S2)}$$

$$g(p)=arctg\left[\frac{x+t_1}{z+t_3}\times\frac{y+t_2}{\sqrt{(x+t_1)^2+(y+t_2)^2+(z+t_3)^2}}\right] \quad \text{(Eq. S3)}$$

where, M was the magnetization of a square magnet (unit: T), t_1, t_2 and t_3 were the coordinates of each vertex of the magnet as shown in fig. S1b, and $g(s)$ represented the component of the magnetic field in each quadrant of the magnet. This formula can be used to calculate the magnetic field component at any position in space. The size of the magnet was 10 cm × 10 cm × 1 cm, the magnetization intensity was 1.4 T, and the height z was 1.5 cm (*i.e.,* the sum of the thickness of the water surface and the petri dish). Therefore, the magnetic field strength at the edge was 2752.5 G. Refer to the magnetic hysteresis loop of Fe_3O_4 nanoparticles (fig. S1c), where the magnetization intensity of Fe_3O_4 nanoparticles was 72 emu g^{-1}. Also, this formula of magnetic field force can be simplified as $F_{magnetic}$ = BHS/2. The area S of the magnet is 0.01 m^2, and the magnetic force exerted by the fiber per unit length of 1 cm was 8.621×10^{-5} mN. At this time, 1.510×10^{3} stacked fibers were required to break through the surface tension of water,

which significantly improved efficiency compared with 9.552×10^6 fibers. As a result, the magnetic assisted electrospinning device used in this work can effectively prepare discrete fiber scaffolds.

To understand the role of Fe_3O_4 in the formation of discrete fiber scaffolds, PAN fibers were fabricated *via* the same approach at various Fe_3O_4 concentrations. It can be seen from the SEM images that when the Fe_3O_4 content was less than 26%, the nanoparticle distribution on the fiber surface was relatively uniform and no obvious agglomeration occurred (fig. S1d-g). However, when the Fe_3O_4 content continued to increase to more than 28%, obvious agglomerated nanoparticles can be observed on the surface of the fiber (fig. S1h and i). These naked nanoparticles were easy to be phagocytosed by cells during cell culture, causing potential cytotoxicity. Therefore, only a proper amount of Fe_3O_4 (26%) can avoid or have less cytotoxicity while yielding the highest average pore size value up to 17.9 μm (fig. S1j). As a result, 26%-Fe_3O_4 PAN (named Fe_3O_4/PAN) fibers were selected as the precursor for the fabrication of bio-NGs.

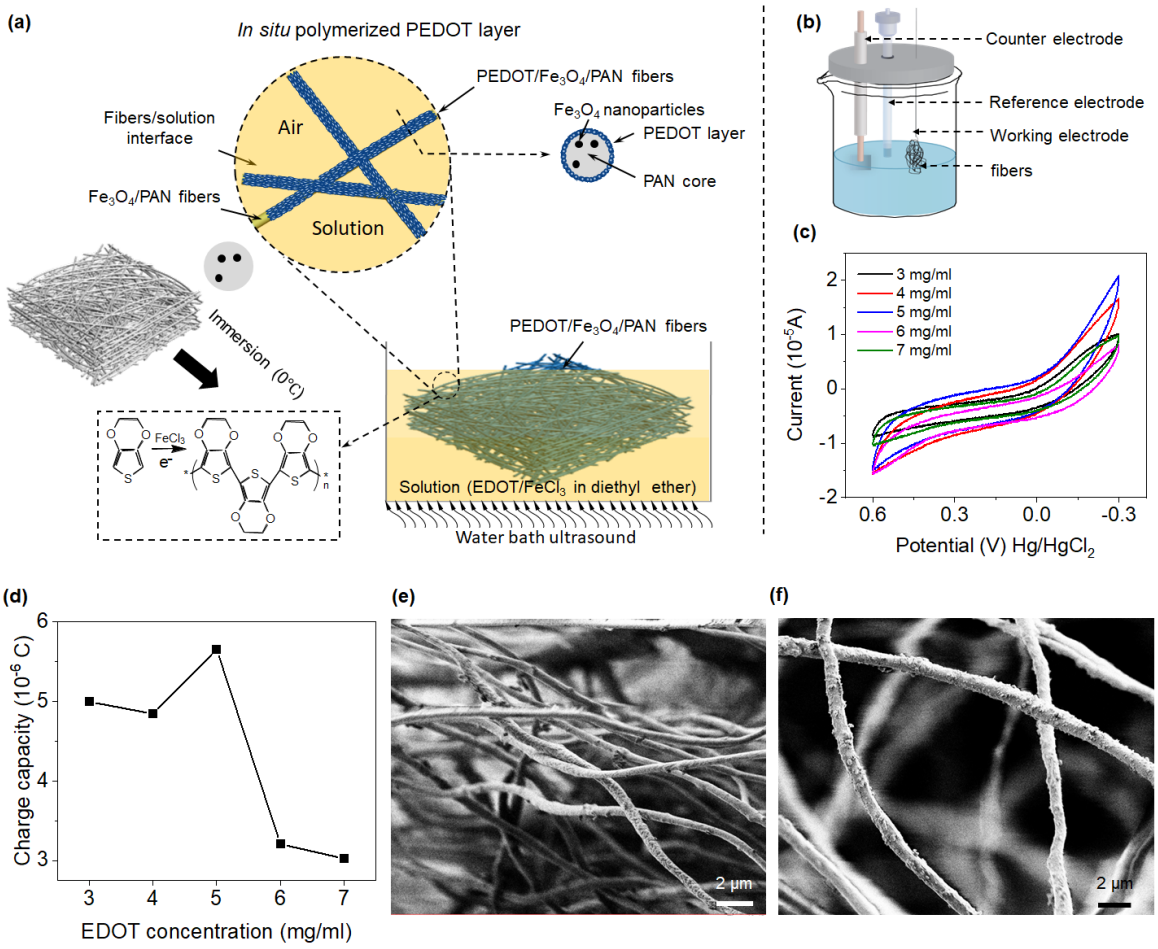

fig. S2. (a) Schematic diagram of the in-situ introduction of PEDOT layer on Fe_3O_4/PAN fibers. (b) Schematic of the three-electrode system for electrochemical performance testing. (c) CVs profiles of Fe_3O_4/PAN fibers with different EDOT concentrations measured in PBS solution. (d) The charge capacity as a function of the EDOT concentration quantified from CV data. When the EDOT concentration was 5 mg/mL, PEDOT/Fe_3O_4/PAN fibers possessed the best charge transfer ability, and its charge capacity was as high as 5.653E-6 C. The SEM images of PEDOT/Fe_3O_4/PAN fibers obtained by (e) ultrasonic reaction bath and (f) static reaction after 35 minutes of reaction at 0 °C. Under ultrasonic reaction conditions, the surface of the PEDOT/Fe_3O_4/PAN fibers was smoother, and the PEDOT layer on the fibers surface was more compact, which was beneficial to the subsequent electrostatic adsorption of GO. Therefore, the ultrasonic reaction was finally selected as the ideal reaction condition.

In this study, the concentration of Fe^{3+} in ethanol was controlled at a very low level (0.02 g mL^{-1}) to prevent EDOT polymerization at the beginning of the process. The Fe^{3+} at the interface between the electrospun fibers led to a fast interfacial polymerization of EDOT to form PEDOT shells on the surface of the electrospun fibers. A three-electrode system was used for CV testing (fig. S2b). All PEDOT-based Fe_3O_4/PAN samples exhibited a highly reversible CV wave form without any obvious side reactions (oxidation and reduction peaks), suggesting a highly

electrochemical stability and no reaction occurred in this scaffold (fig. S2c). The area of the closed CV curves, an important parameter in the electrochemical reaction, can be used to evaluate the charge amount passed on the scaffold, where the 5 mg mL^{-1}-EDOT Fe_3O_4/PAN (named PEDOT/Fe_3O_4/PAN) fibers gave the highest charge capacity value of 5.653E-6 C (fig. S2d). Therefore, we choose this EDOT concentration as the precursor for fabricating bio-NGs.

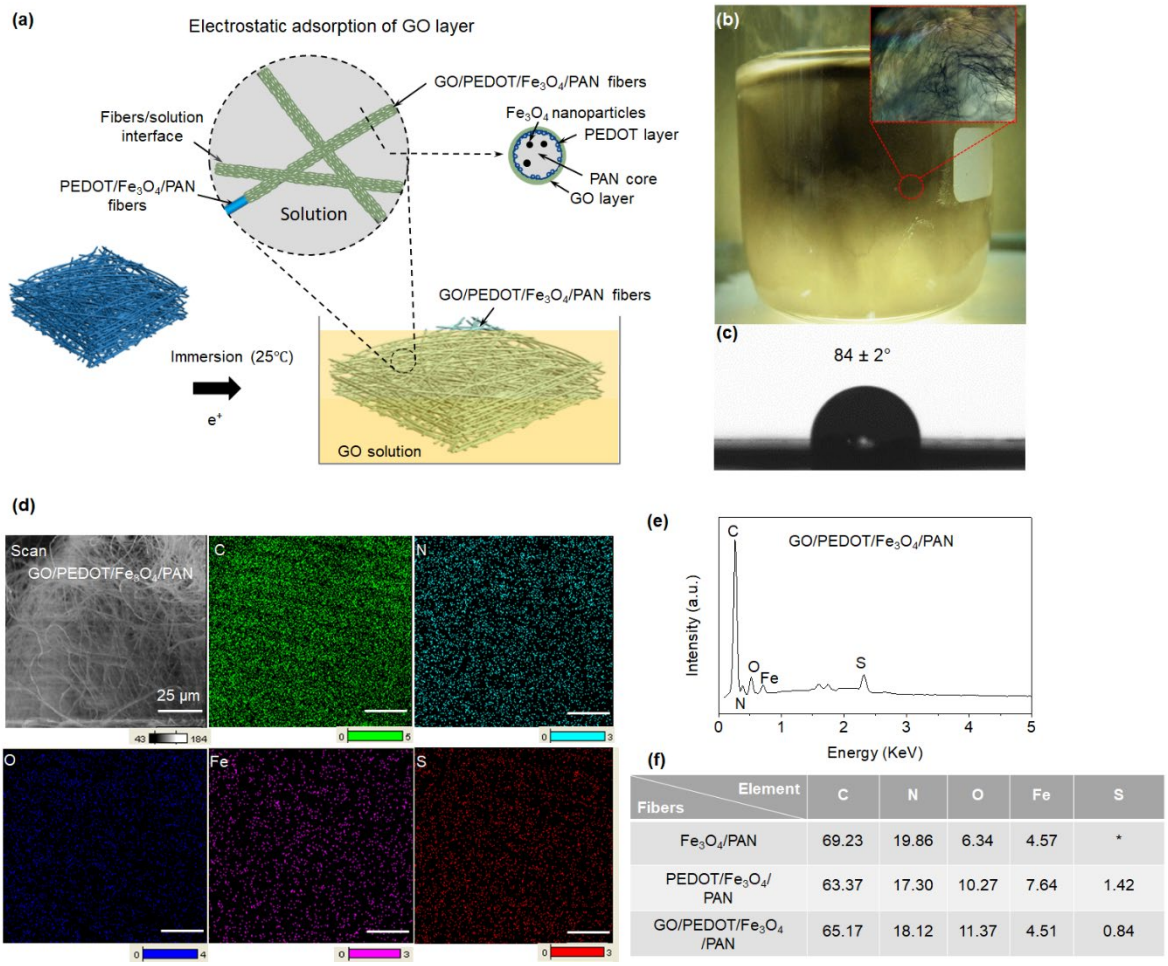

Fibers \ Element	C	N	O	Fe	S
Fe_3O_4/PAN	69.23	19.86	6.34	4.57	*
PEDOT/Fe_3O_4/PAN	63.37	17.30	10.27	7.64	1.42
GO/PEDOT/Fe_3O_4/PAN	65.17	18.12	11.37	4.51	0.84

fig. S3. (a) Schematic diagram of introducing GO layer on PEDOT/Fe_3O_4/PAN fibers by electrostatic adsorption. (b) Optical image of highly discrete GO/PEDOT/Fe_3O_4/PAN fibers. (c) Water contact angle image of GO/PEDOT/Fe_3O_4/PAN fibers. (d) EDS mapping of GO/PEDOT/Fe_3O_4/PAN fibers. (e) EDS profiles of C, N, O, Fe and S elements in GO/PEDOT/Fe_3O_4/PAN Fibers. (f) The proportion of atoms in different PAN-based fiber scaffolds. Photo credit: Chuanmei Shi, Nanjing University of Science and Technology.

3D GO/PEDOT/Fe_3O_4/PAN fibers were obtained by immersing freeze-dried PEDOT/Fe_3O_4/PAN fibers in GO solution with a concentration of 5 mg mL^{-1}. While the surface of GO was rich in anionic groups such as carboxyl and hydroxyl groups, which can be electrostatically adsorbed with PEDOT, thereby self-assembled into GO outer layer. Obviously, EDS mapping and EDS profiles supporting the presence of Fe_3O_4, PEDOT and GO in bio-NGs.

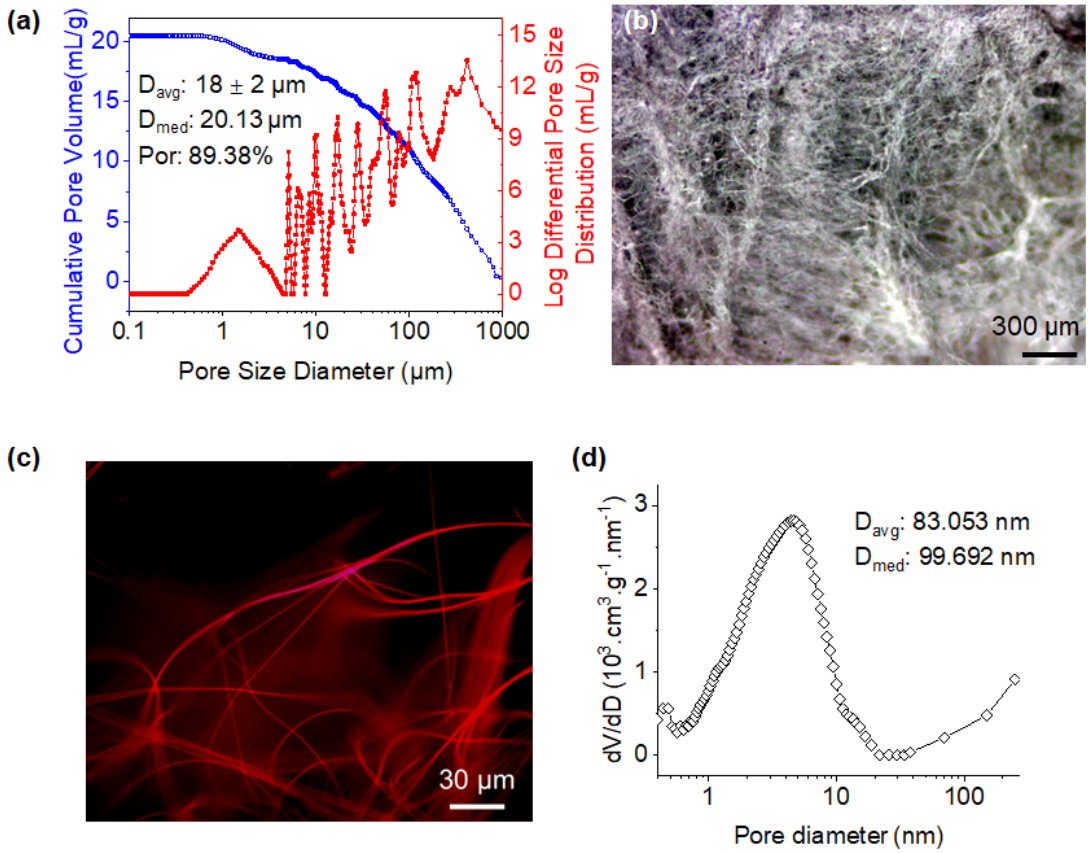

fig. S4. (a) MIP cumulative pore volumes (blue) and the associated derivative pore volume (right) of Fe_3O_4/PAN fibers as a function of pore size diameter. (b) The high-resolution stereo microscope image of the target fibers showing many gaps induced by the interlacing of the fibers. (c) Laser scanning confocal image showing highly discrete target fibers. Red: Rhodamine B. (d) Pore size distribution of the target fibers. The micropore size distribution was obtained by the Dubinin-Astakhov method. The mesopore size distribution was calculated by the Brunauer-Emmett-Teller method.

As shown in revised Fig. S4a, the porosity of our target fiber scaffold is as high as 89.38%. Moreover, the average pore size is 16.72 μm, which is slightly smaller than that (18 μm) measured by ImageJ but still within an acceptable error range. This may be caused by the compression of the fiber scaffold by the inherent pressures during MIP (0.8-30000 psia). We also found that this target scaffold has a wide range of pore size distribution. In general, the median pore size can be used to quantify the pore size distribution. Notably, the median pore size is as high as 20.13 μm. In parallel, these large pores in the scaffold can be clearly observed through high-resolution stereo microscope and laser scanning confocal images (Fig. S4b and c). Therefore, for an objective and comprehensive evaluation of our bio-NGs, we marked the pore

size as 18 ± 2 μm. From the above results, it is clear that our target scaffold can ensure that cells migrate smoothly into the scaffold to form a cell-3D culture microenvironment.

On the other hand, generally speaking, the MIP is suitable for the characterization of pores >200 nm, while the nitrogen adsorption method is commonly used to characterize pores <100 nm. Therefore, to fully evaluate our fiber scaffolds, we also tried to use the nitrogen adsorption method to characterize the micro/mesopores in the scaffold with a size of less than 100 nm. Obviously, many micro/mesopores < 100 nm existed in this target scaffold (Fig. S4d), which could promote cell interaction/adhesion with fibers. In summary, our target fiber scaffold has a large enough pore size for cells to enter, and the nanotopological structure formed by these micro/mesopores is also conducive to cell adhesion.

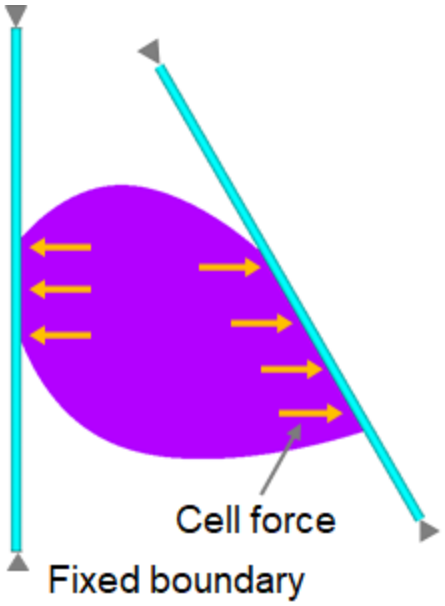

fig. S5. The physical model of two PAN fibers coupled with a living cell, and the boundary conditions were considered as fixed constraints at both ends of fibers.

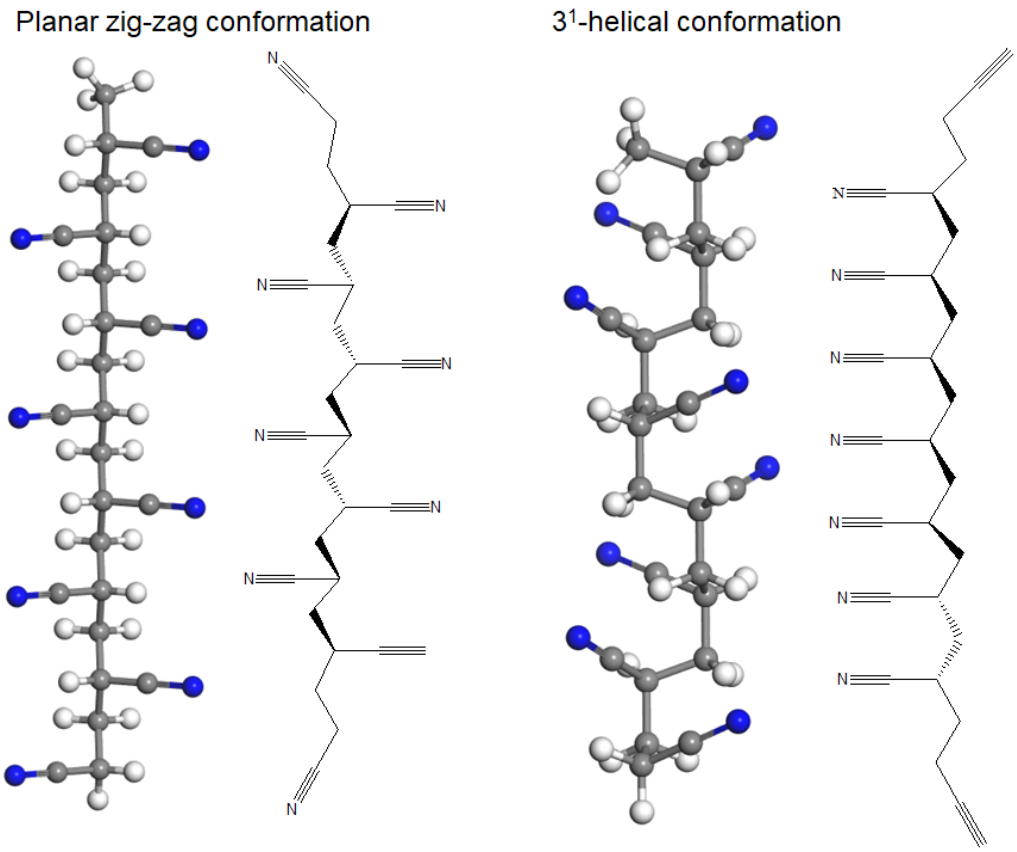

fig. S6. Planar zig-zag conformation of PAN and 3^1-helical conformation of PAN.

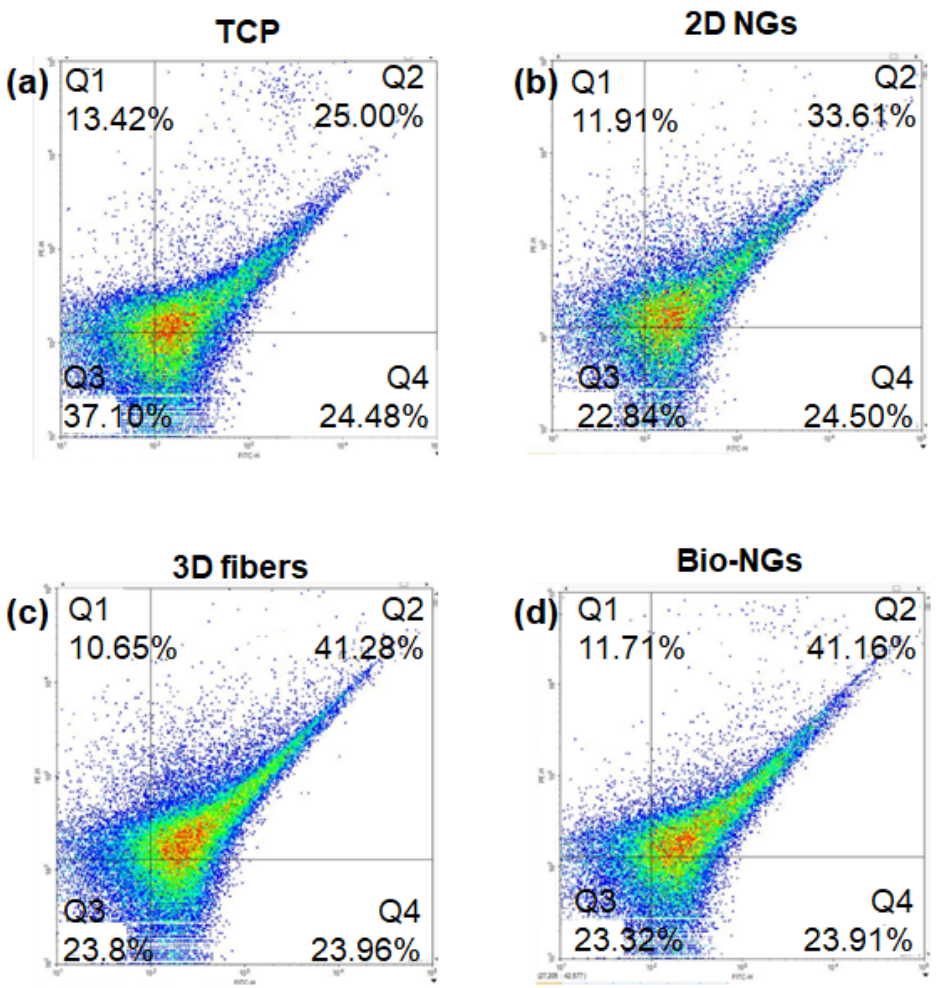

fig. S7. Apoptosis images of RGC5 neurons after 5 days cultured in (a) TCP, (b) 2D NGs, (c) 3D fibers and (d) bio-NGs.

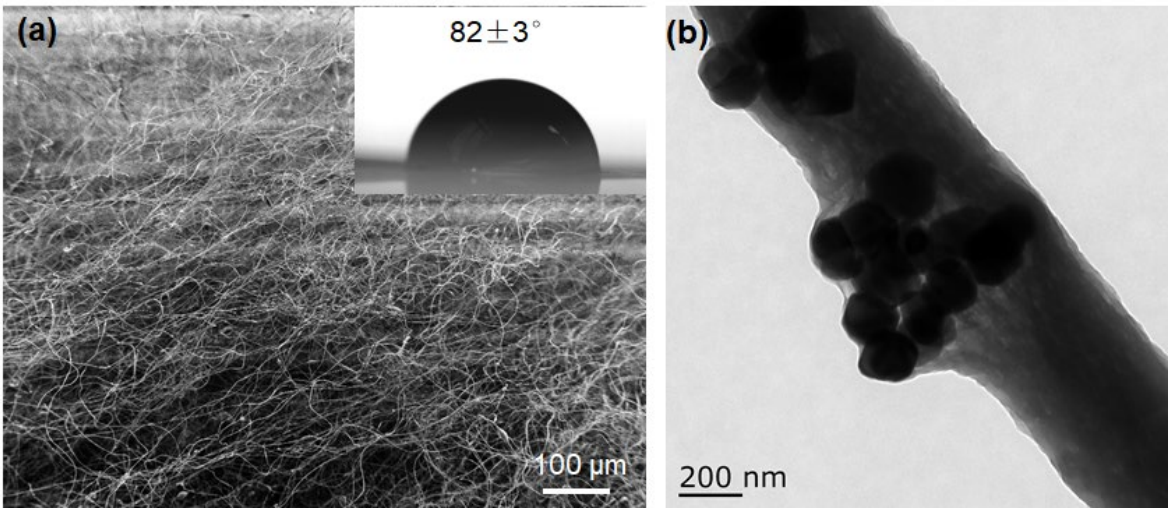

fig. S8. (a) SEM and (b) TEM images of 3D fibers. The inset of (a) showed that the water contact angle of 3D fibers is 82 ± 3°.

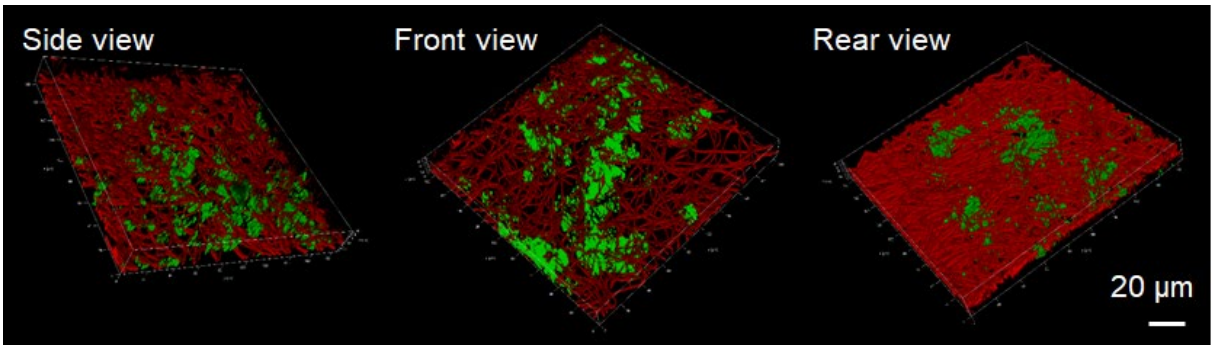

fig. S9. 3D confocal scanning of RGC5 neurons cultured in 3D fibers from different perspectives.

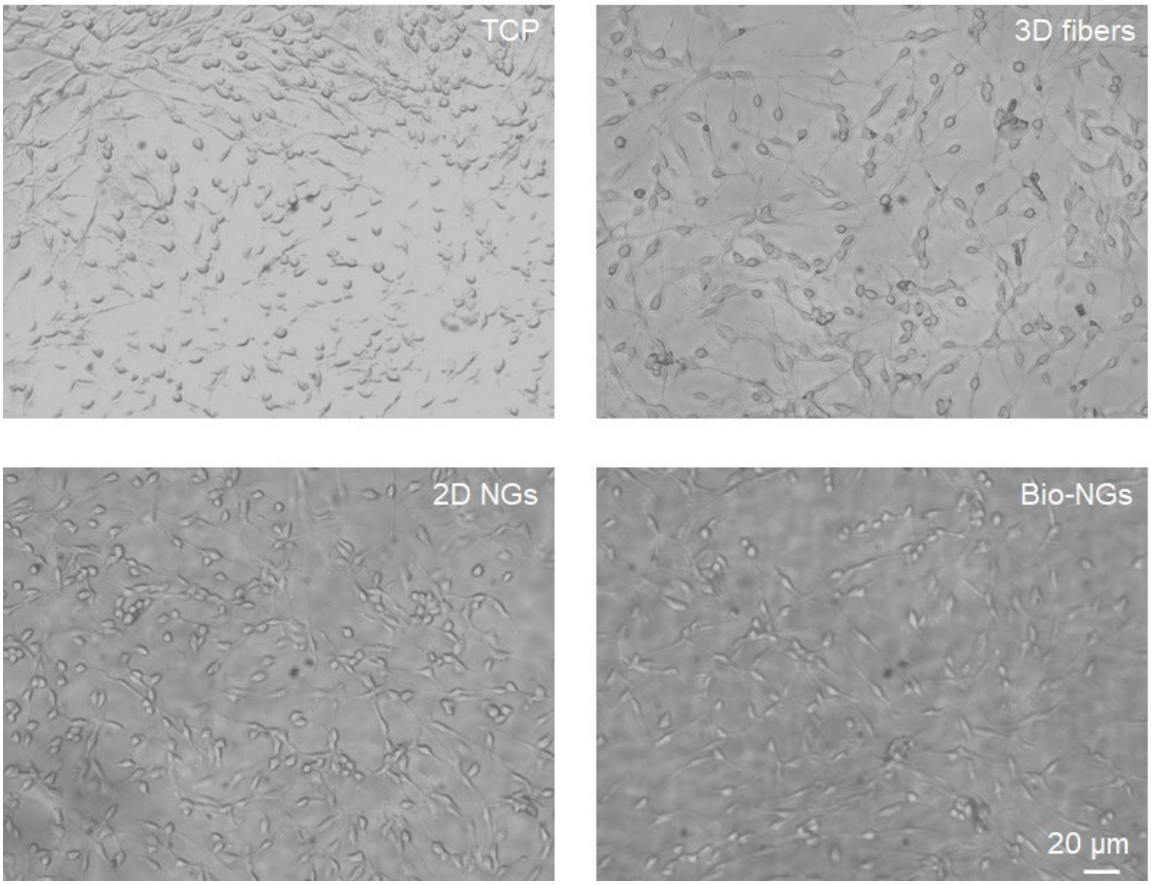

fig. S10. Optical images of RGC5 neurons after 5 days cultured on TCP, 2D NGs, 3D fibers and bio-NGs.

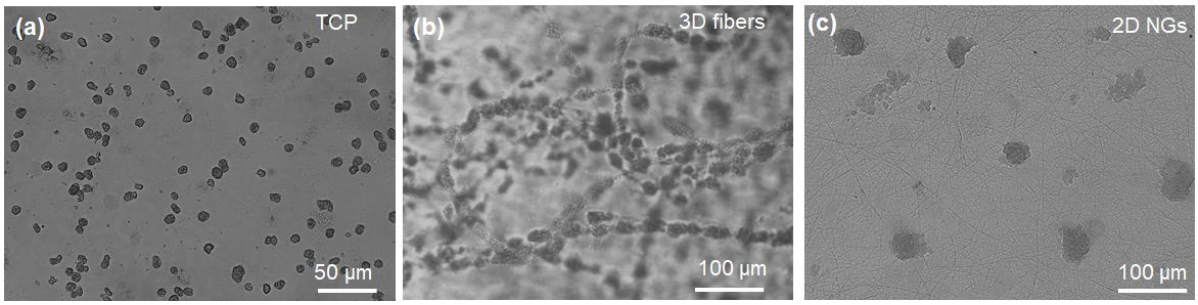

fig. S11. Light microscope images of primary hepatocytes cultured on (a) TCP, (b) 3D fibers and (c) 2D NGs, respectively.

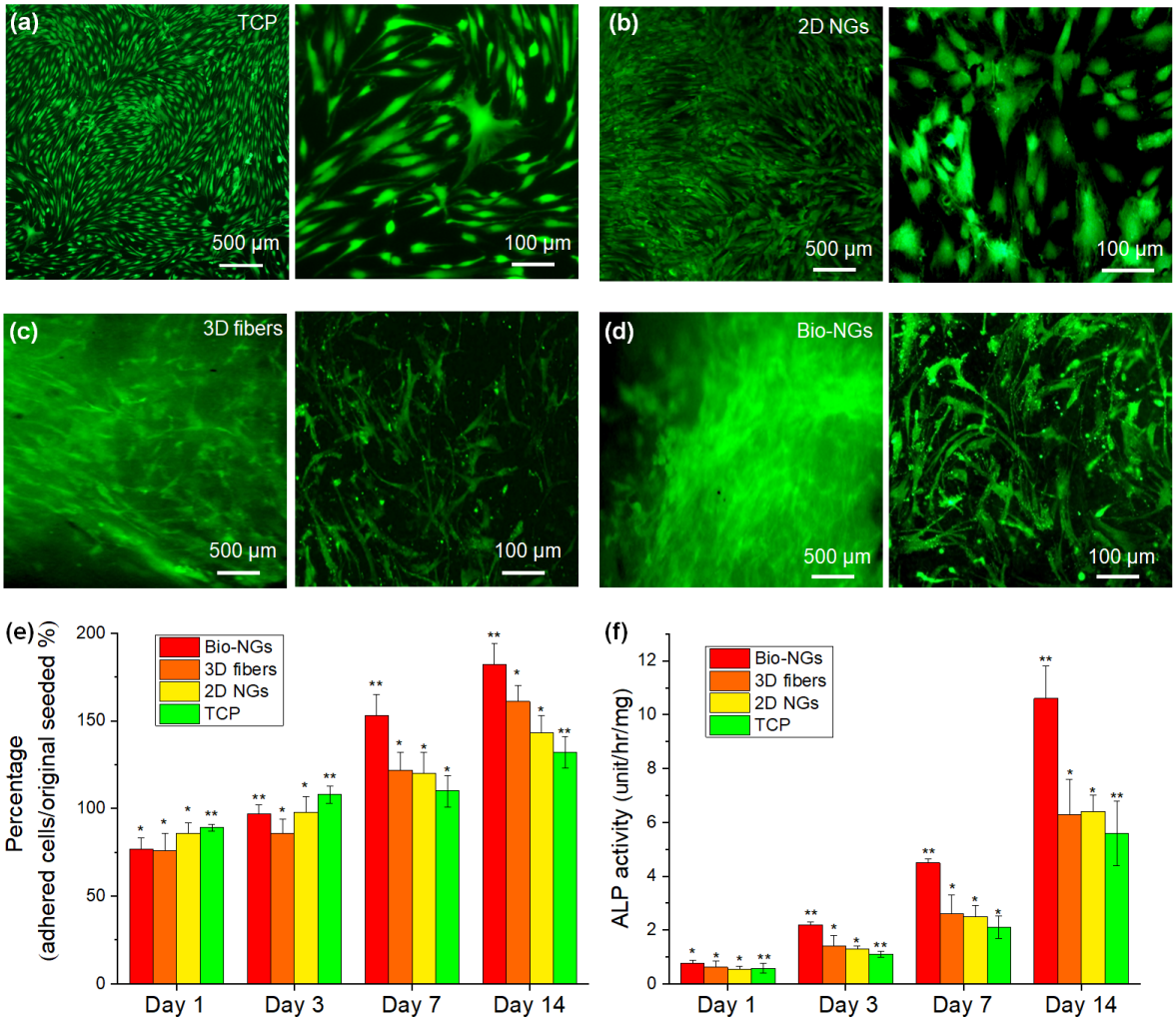

fig. S12. FDA fluorescence images of hMSCs cultured on (a) TCP, (b) 2D NGs, (c) nonpieoelectric 3D fibers and (d) bio-NGs for 14 days. (e) Proliferation rate of hMSCs by the DNA assay on day 1, day 3, day 7 and day 14. (f) The early osteogenic markers: ALP activity evaluation of hMSCs. All error bars indicate ± s.d. n=3, $*P < 0.05$, $**P < 0.01$.

Electric stimulation is well recognized as an effective method to elicit osteogenic differentiation of stem/progenitor cells and bone formation. On these grounds, various forms of electric stimulation are widely used clinically to enhance bone healing and treat fracture nonunion. Therefore, we added a new set of cell lines to culture *in vitro* to further evaluate bio-NG-cell interaction — human mesenchymal stem cells (hMSCs) differentiate into osteoblasts. For the specific process of hMSCs culture and its osteogenic differentiation characterizations, please refer to Note S7. To clearly observe the differentiation morphology of the cells, the hMSCs were fluorescently stained with fluorescein diacetate (FDA). When performing a fluorescence microscope scan, FDA was excited by a laser with a wavelength of 484 nm to

highlight the hMSCs morphology (Fig. S12a-d). hMSCs cultured in 3D scaffolds including bio-NGs and 3D fibers exhibited a higher level of cell spreading. From the magnified view of the FDA fluorescent staining images, 3D fibers and bio-NGs induced cell attachment with a more spread morphology compared to 2D scaffolds (*i.e.,* TCP and 2D NGs). Notably, hMSCs displayed flattened and polygonal-shaped morphology with large cell body extension along the fibers, especially in bio-NGs. Such morphology in bio-NGs, analogous to the features of osteoblasts indicated the early onset of differentiation. Next, to quantify these substantial differences in cell spreading, we calculated the cell proliferation rate adhered to different scaffolds using DNA assay. The cell proliferation rate was obtained by dividing the adhered cells by the original seeded cells. Starting from day 7, the cells cultured in bio-NGs displayed the highest proliferation rate as shown in Fig. S12e. This meant excellent cell adhesion, matching well to the results of fluorescent staining images, which was conducive to the transmission of intracellular tension to the piezoelectric fibers in bio-NGs. Overall, such a flattened and polygonal-shaped morphology of hMSCs in bio-NGs, analogous to the features of osteoblasts indicated the early onset of differentiation. Finally, to confirm the osteoblastic differentiation, the activity of alkaline phosphatase (ALP), one of the early osteogenic markers, was evaluated to investigate the differentiation patterns of hMSCs cultured on piezoelectric fibers in 3D space (*i.e.,* bio-NGs). As the typical characteristic nature of osteoblastic differentiation, a temporal rise and fall in ALP activity was recorded in all experimental groups (Fig. S12f). Almost at each time point studied, the ALP activity of hMSCs was significantly higher in bio-NGs, when compared to the other scaffolds (*i.e.,* TCP, 2D NGs and 3D fibers). Notably, there was no statistically significant difference in ALP level between 3D fibers and 2D NGs, but both were significantly larger than that of TCP. This indicated that both NG-cell interaction and 3D space could induce osteoblast differentiation. Moreover, the highest level of ALP activity was recorded on bio-NGs on day 14. From the above data, it is obvious that the 3D cell growth space coupled with NG-cell interactions in bio-NGs further promote the differentiation of osteoblasts.

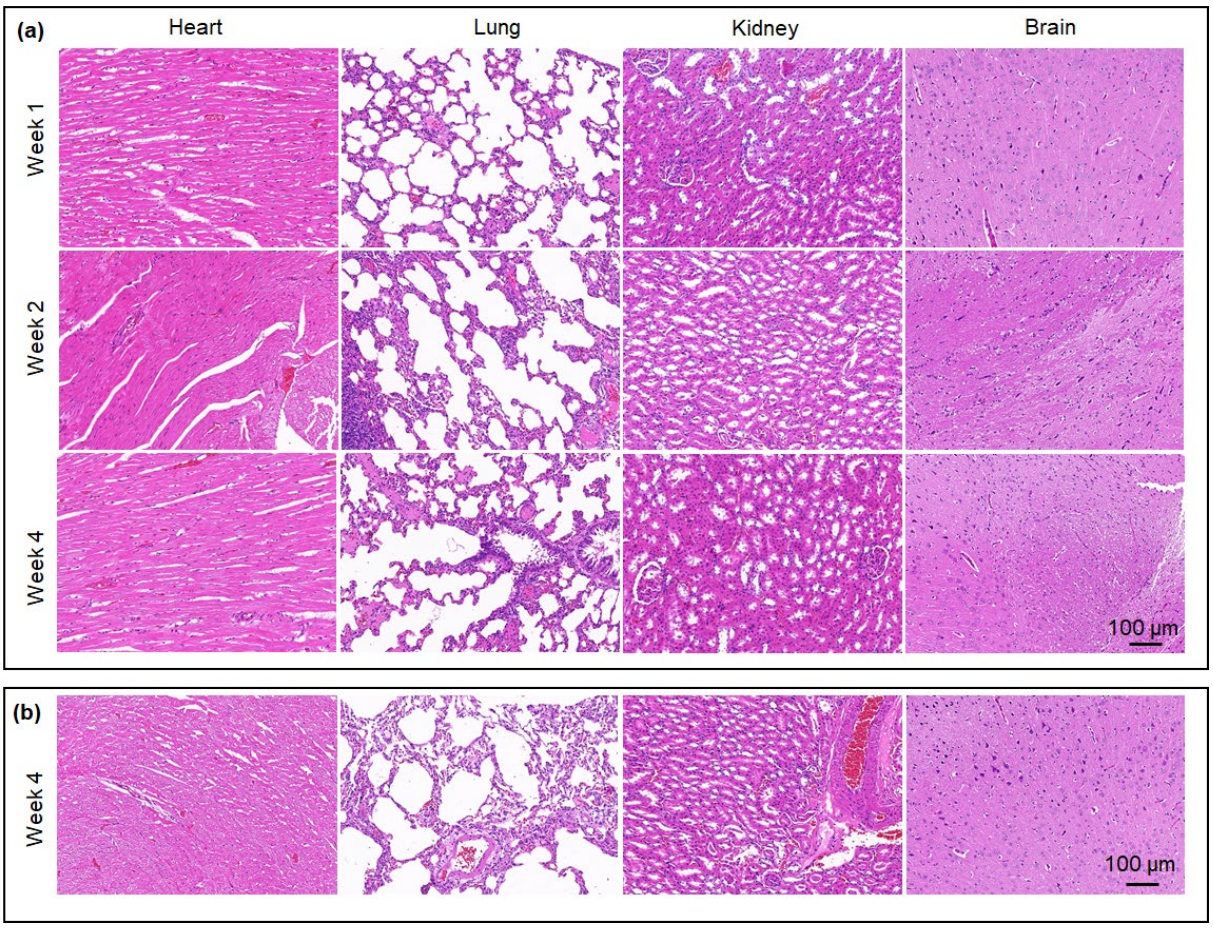

fig. S13. (a) H&E staining of vital organs (heart, lung, kidney, and brain) at different time points (week 1, week 2, and week 4) after bio-NGs implantation. (b) H&E staining of vital organs (heart, lung, kidney, and brain) after the 4th week of 3D fibers implantation.

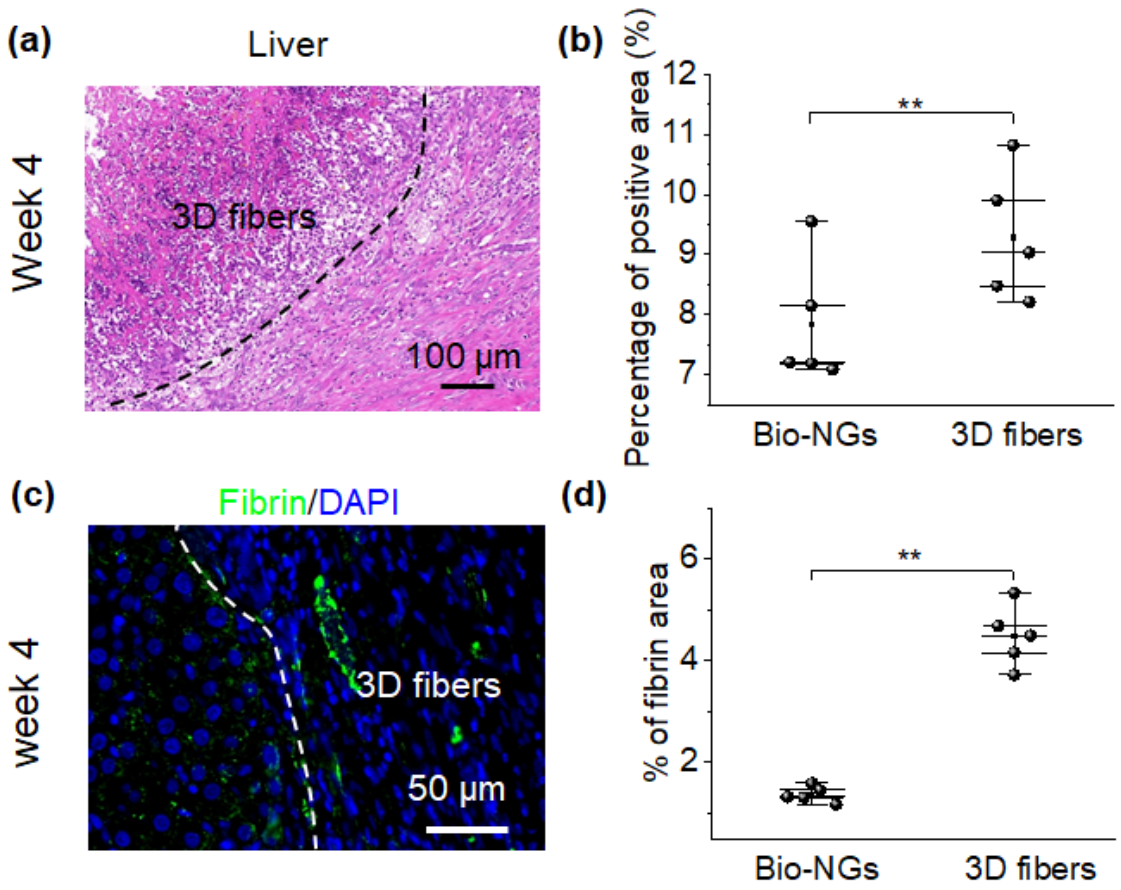

fig. S14. (a) H&E staining of the liver sections at 4th week of 3D fibers implantation. (b) Quantification of the percentage of positive area showing a weaker inflammation in bio-NGs than 3D fibers. (c) Representative images of hepatic fibrin(ogen) immunostaining (green) in DAPI (blue)-counterstained liver sections at 4th week of 3D fibers implantation. (d) Quantification of hepatic fibrin immunostaining showing less fibrin deposition in bio-NGs than 3D fibers. Data are expressed as mean values ± S.D. n = 5, $^{**}P < 0.01$.

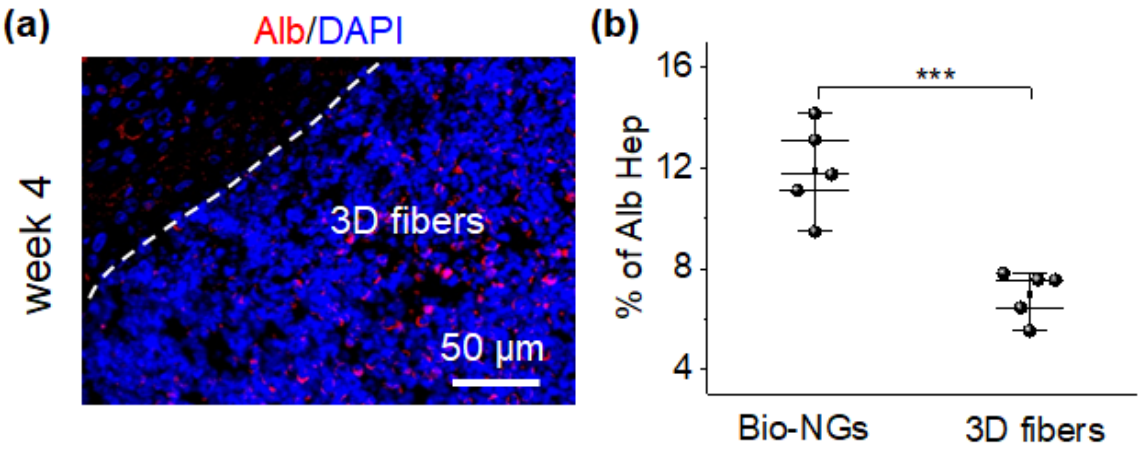

fig. S15. (a) Immunostaining for Alb (red) on liver sections at 4th week of 3D fibers implantation. (b) Quantification of the percentage hepatocytes expressing Alb showing higher Alb expression level in bio-NGs than 3D fibers. Data are expressed as mean values ± S.D. n = 5, ***$P < 0.001$.

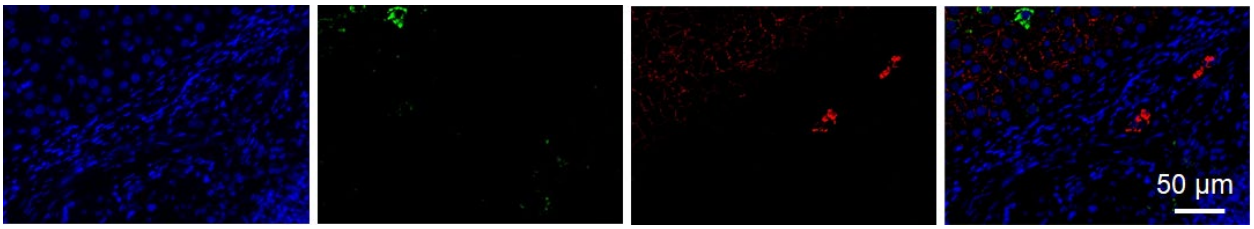

fig. S16. Immunostaining for GS (green) and E-CAD (red) on liver sections at 4th week of 3D fibers implantation.

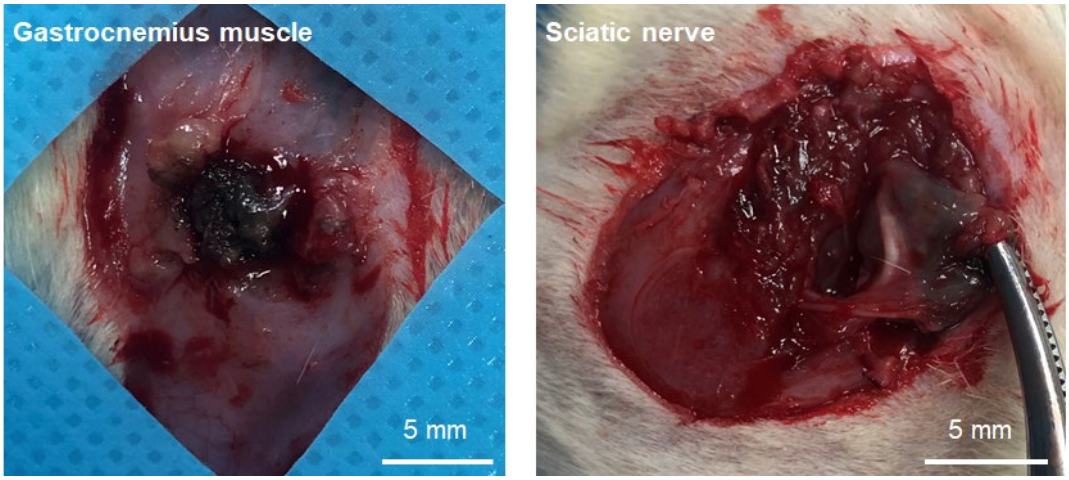

fig. S17. Surgical images of the implanted bio-NGs after 8 weeks. The implants were packaged by surrounding tissue, and the tissue inflammation and festering did not occur after the postoperative 8 weeks. Photo credit: Tong Li, Nanjing University of Science and Technology.

Supplementary Table

table S1. The diameter of fibrous ECM components and the fibers in bio-NGs.

Component	Diameter
Fibers in Bio-NGs	**400-900 nm**
Collagen fibrils	**10-500 nm**
Collagen fibril bundles	**0.5-10 µm**
Elastin fibrils/fibers	100-200 nm
Laminin fibrils/fibers	20-100 nm
Fibronectin fibrils/fibers	2-20 nm

table S2. Overview of cell size of different cell types.

Cell type	Diameter (μm)
Monocyte	7-10
Neutrophil	8-10
Exocrine cell	9-15
Fibroblast	10-15
Stem cell	6-18
Osteocyte	5-20
Lymphocyte	7-20
Tissue cell	10-20
Macrophage	21
Cardiomyocyte	10-25
Hepatocyte	15-30
Muscle cell	10-50
Hela	20-40
Osteoblast	15-50
Adipocytes	70-120